

**CHAPTER II:**  
**MATERIALS AND METHODS**

## **II.1. Tools**

At the beginning of this study a regional synthesis was compiled, using all available information from the literature, including published and property surface and sub-surface sections, geological and structural maps for Fars, Bandar Abbas and West High Zagros.

### **II.1.1. Existing data:**

A total of 6 outcrop sections and 15 subsurface wells from the zagros area, containing paleontological, Gamma Ray and Sonic/Density logs, were available in the NIOC archives. Data were used to prepare a series of regional transects. The former surface sections and logs employed in transects were redrawn. The main Palaeozoic litho-stratigraphic surface and subsurface sections in the Zagros are listed in the [Table I. 1](#).

### **II.1.2. Field trips:**

In total two field surveys were carried out in the Bandar Abbas (Kuh e Faraghan and Kuh e Gahkum) and in the Fars (Kuh-e- Surmeh) areas. During the fieldwork, the sedimentary structures, lateral variations and depositional geometries were studied in detail. In addition special emphasis was placed on detecting sequence stratigraphic parameters such as stacking patterns and characteristic surfaces. The average sampling interval is less than 3 m.

### **II.1.3. Thin sections:**

A total of 270 samples were collected from Kuh e Gahkum, Kuh e Faraghan and Kuh e Surmeh and 5000 core drilled thin sections, have been studied, for petrofacies analysis.

### **II.1.4. X-ray diffraction:**

Clay minerals are useful tools for studying provenance of the sediments and paleoclimatic conditions in the source area and of the sediments. They can also give information about the burial history of sediments ([Moore & Reynolds, 1997](#)). A total 200 samples were collected for X- ray Diffraction analysis to distinguish of clay minerals. This contribution concentrates on the distribution of clay mineral assemblages in the Palaeozoic succession at the Kuh e Faraghan, Kuh e Gahkum and kuh e Surmeh.

All samples are first cleaned and crushed in order to retain the unaltered portions. Products crushing are dried in an oven at low temperature (<40° C) and ground to a fine powder manually with a mortar and pestle. The particle size fraction of clay samples (<2 microns) is then isolated and prepared blades oriented in the detailed Protocol [Holtzapffel \(1985\)](#). A decarbonation is first performed by etching with hydrochloric acid N/5, stirring magnetic. Five to ten cycles of decanting / rinsing allow removal of excess acid and deflocculation of clay minerals. Samples were transferred to measuring cylinders and the clay fraction (less than 2 microns) was isolated from the coarser fraction by the Atterberg method (settling time based on Stoke's Law).

After micro- homogenisation, the sample settles to rest for 1h35min. Fraction of clays less than 2 microns, focused on the top two centimeters of suspension is imposed syringe. Centrifugation at 3500 rpm for 40 min to allow the solution collected obtain a concentrated clay pellet. Each preparation led to the making of two oriented slides.

DRX is applied to the thin slides having undergone three types of processing (Moore & Reynolds, 1997):

- Treatment (Natural drying of the sample at room temperature)
- Saturation in ethylene glycol for 6 hours, so as to vary the thickness of the field interlayer swelling clays
- Heating the oven to 490° C for 2h after 1h temperature rise to disrupt kaolinite, whose characteristic peaks disappear above this temperature , which allows the differentiate correctly chlorite, some of which are common peaks with kaolinite .

The slides are then analyzed by a diffractometer Bruker D4 Endeavor ®, using an anode Type -  $K\alpha_1$  Cu, a filter of Ni, and a detector LynxEye generator operating at a voltage of 40 kV at an intensity of 25 mA. The goniometer of the diffractometer allows a rotation of 2.5 to 28.5 ° with a step of 0.0399 ° for 11 min 34 s and a speed of 15 rotations per minute, for three tests. The result is the production of three diffractograms per sample (Fig. II.1).

The diffractograms are in the form of a series of localized peaks at angles specific to each mineral species reflection. These reflection angles are converted to thicknesses by Bragg's law. Each mineral species has a basal reflection peak, denoted (001) matching the interlayer space. The following peaks, denoted (002), (003), etc. Correspond to harmonics and reflection are located on integer multiples of the basal reflection. For example illite has a peak (001) located at 10 Å. Harmonics (002) and (003) illite are then localized 5 respectively and 3.33 Å.

The diffractograms are analyzed under MacDiff software (version 4.2.5; Petschick, 2000). The semi-quantification of minerals in the presence is checked by measurement of area, rather than by measures peak intensity on glycolated samples where the reflections are more widely spaced (Holtzapffel, 1985; Moore & Reynolds, 1997).

We could identify the four main clay mineral groups: illite, chlorite, illite/smectite, and kaolinite in the sediments of the Productive Series.

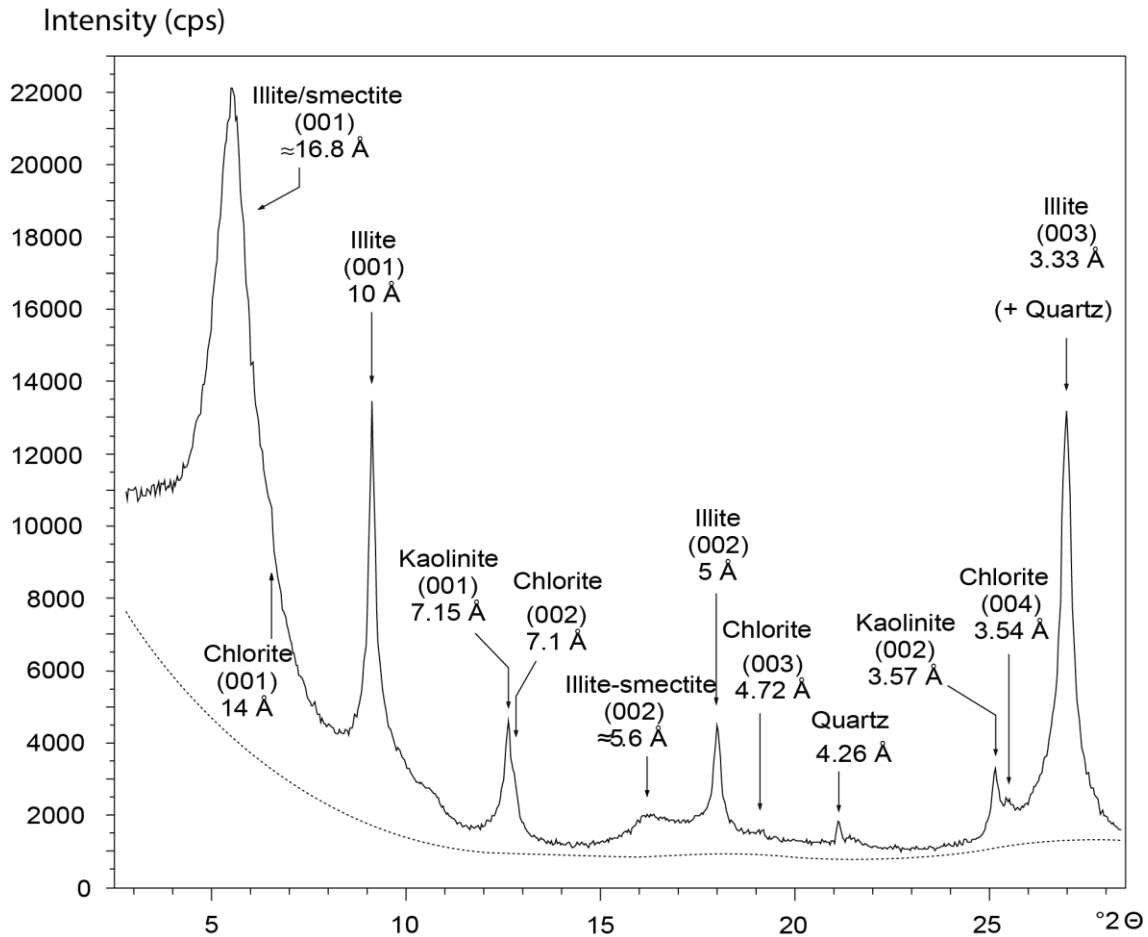


**Fig. II.1:** Example of diffraction of a glycol blade with location of the reflection peaks of the main species clay minerals (Moiroud et al., 2012).

### II.1.5. Gamma-ray:

The measurements are performed in situ spectral gamma-ray with a spectrometer cell SatisGeo® GS -512 (Fig. II.2). It consists of a probe with a diameter of 12 cm connected by a cable to a unit station that records the measurements. The probe is equipped with a scintillation detector GSP- 3 provided a crystal of NaI (Tl). During a constant acquisition time of one minute, the scintillator captures each gamma radiation and amplifies its signal. The latter is then converted into an electrical signal and counted by the CPU, which can measure the surrounding radioactivity. Each source radioactivity emits its own energy band. The device is designed to separate each band energy, which helps to distinguish the source of energy emitted by the rock ( $^{40}\text{K}$ ,  $^{238}\text{U}$  and  $^{232}\text{Th}$ ) noise background caused by cosmic interaction / atmosphere radiation or by anthropogenic pollution. In from these measurements, the CPU calculates the concentration of these three elements, expressed in % for ppm potassium and uranium and thorium. The amount of total





radiation is expressed as ppm equivalent uranium (eU ppm, 1 ppm = 1 $\mu$ g / g; SatisGeo <sup>®</sup>, instruction manual)



**Fig. II.2:** Measurement of gamma-ray with GS-512.

The camera captures 90% of its signal over a radius of about 20 cm (Vacek et al., 2010). Of biases effects to the measured surface flatness exist. If the measured surface is located in a cavity, the " overflow " of material around the probe leads to an overestimation of the value of spectral gamma-ray. Conversely, if the measurement is done on a projection (eg, on a very resistant limestone bed erosion compared marls that frame), the lack of material around the projection leads to an underestimation of the value of spectral gamma-ray. The measurements are taken at the most possible planar surfaces. The marl is routinely updated so as to measure the marl interbank targeted and no alteration products. Precautions are taken to obtain flat surfaces after refresh cutting. Measuring 30 times the same sample of sandstones and shales tested the reproducibility of the measurements.






In this study, we used different scales for gamma-ray and amount of uranium, potassium and thorium (Table II.1).

Logs	GR(API)	U(ppm)	TR(ppm)	K(ppm)
Scales				

**Table II.1:** The scales of spectral gamma-ray logs. We used different scales for gamma-ray and amount of uranium, potassium and thorium.

The gamma-ray log is an useful tool for discrimination of different lithologies. Its main use is the discrimination of shales and organig rich shales by their high radioactivity. By contrast, clean sandstones, dolomites and limestones have low gamma ray values.

The principle gamma-ray log shapes are frequently used for interpreting sedimentary cycles or depositional facies. The five log trends (**Table II.2**) are bell shape (upwards increasing in gamma counts), funnel shape (upward decrease in gamma counts), box-car or cylindrical (relatively consistent gamma readings), bow shape (systematic increase and decrease of gamma counts) and irregular trend (no systematic change in gamma values) (Cant, 1992; Reader, 1993). The shape of the curves can also assist in determining the depositional environment. For example, boxcar-, funnel- and bell-shaped patterns of gamma logs can be correlated with beach sands, prograding barrier islands and intertidal point bars, respectively (**Table II.2**).

Shapes	Boxcar	Funnel	Bell	Symmetric	Irregular
Gamma-Ray logs					
Gomma counts	Relatively consisting gamma ray reading	Upward decreasing	Upward increasing	systematic increasing and decreasing	no systematic changes
Sequences	Uniform	Finning upward	Coarsening upward	Coarsening and finning upward	Intercalation
Depositional environments	Beach sand Aeolian sand Evaporite	Barrier island Crevasse splay Mouth bar	Point bar Marine channel Tidal creek	Offshore shoal Trangressive-sands	Flood plain Tidal flat Marsh

**Table II.2:** The gamma ray log and depositional environments (after Cant 1992; Reader, 1993). These informations used to interpretation of lithology, facies, depositional environments and depositional sequences

In this study, the gamma ray of 1200 m thick of the Palaeozoic succession were measured for the first time in three outcrop sections (Kuh e Gahkum, Kuh e Faraghan and Kuh e Surmeh). These data is used to correlation with 11 subsurfaces sections in studied area containing of gamma ray and sonic/density logs. These informations used to interpretation of lithology, facies, depositional environments and depositional sequences.

### II.1.6. Biostratigraphy:

Since 1984, more than 1000 surface and subsurface samples from the Palaeozoic succession were examined for palynomorph entites, in order to determine the stratigraphical age of these rock units by Pr. Ghavidel Syooki .The objectives of those studies are to summarized the known stratigraphic range of acritarch assemblages and species from Cambrian up to Permian. These studies confirm that despite of abundant brachiopod, trilobite and graptolite fauna in the Barut,

Zaigun and Lalun Formations (Setudehnia, 1975), these are barren in palynomorph entities (Gahvidel Syooki, 1996). The rest of Palaeozoic (Ordovician to Permian) succession of the Zagros Basin contains rich and well-preserved acritarchs (Gahvidel Syooki, 1996).

Nevertheless, detailed palynological studies in recent three decades by Pr. Ghavidel Syooki, carried out in surface sections (Kuh e Faraghan, Kuh e Gahkum, Kuh e Surmeh, Zard kuh, Chali sheh) as well as subsurface sections (well Dalan#1, well Kuh e Siah#1, well Golshan#3, well Kabir Kuh#1; well Finu#1, well Namak#1, well Zirreh#1, well Naura#1, well Darang#1), have resulted in precise biozonation and age determination of the Palaeozoic rock units in the Zagros area (Fig. II.3).

In this study, we used the Palynological informations of the surface and subsurface sections, to datation and establishing the age relationships and correlation of Palaeozoic succession and its depositional sequences.



ERA	PERIOD	EPOCH	STAGE	ZAGROS ROCK UNIT	Biozone (Ghavidel Syooki, 1995, 1996, 2003, 2008, 2011)	Geodynamic, Climate and Eustatism events (Ghavidel syooki et al., 2011; Konert et al., 2001; Sharland et al., 2001; Al-Sharhan and Nairn, 1997; Frakes et al., 1992; McGillivray and Al-Husseini, 1992; Berberian and King, 1981; Vail et al., 1977)	
(Gradestein et al., 2012)							
PALEOZOIC	Permian	Late	Changhsingian	Dalan Fm.	Pollen/spore Ass. Zone P1 (Hamipollenites-Vittatina)	Zagros Rift and Carbonate transgression	PASSIVE MARGIN
			Wuchiapingian				
		Middle	Capitanian				
			Wordian				
		Early	Roadian				
			Kungurian				
	Artinskian		Faraghan Fm.				
	Sakmarian						
	Carboniferous	Pennsylvanian	Asselian	Zakeen Fm.	Acritarch Ass. Zone D1 (Chomotriletes vedugensis) ; Spore Ass. Zone VI	Global warming Rising sea level	
			Gzhelian				
			Kasimovian				
			Moscovian				
		Mississippian	Bashkirian				
			Serpukhovian				
	Devonian	Late	Visean	Zakeen Fm.	Spore Ass. Zone IV-V	Global warming Rising sea level	
			Turnaisian				
			Famennian				
		Middle	Emsian				
			Eifelian				
Givetian							
Early	Pragian						
	Lochkovian						
Silurian	Lianoverly		Sarchahan Fm.	Acritarch Ass. Zone S2 (Dactylofusa estillis)	Deglaciation - Global warming Rising sea level		
				Acritarch Ass. Zone S1 (Dictyotidium faviformis)			
				Acritarch and Chitinozoan Ass. Zone	Hirnantian Glaciation-Falling sea level		
Ordovician	Late	Hirnantian	Dargaz Fm.	Acritarch Ass. Zone O6	Acritarch Ass. Zone (IV)	Global peaked sea level	
		Katian	Seyahou Fm.	Acritarch Ass. Zone O5 (Villosacapsula actinotodissus)	Acritarch Ass. Zone (I-III) Chitinozoan Ass. Zone (C1-C3)		
	Middle	Darriwillian		Acritarch Ass. Zone O4 (Coryphidium bohemicum)			
		Dapingian	Zardkuh Fm.	Acritarch Ass. Zone O3 (Striatotheca principalis)			
	Early	Floian		Acritarch Ass. Zone O2 (Arbusculidium-Acanthodaicrodium)			
		Tremadocian					
Cambrian	Furongian		Ilebek Fm.	Acritarch Ass. Zone III-IV		Global Rising sea level- Intracratonic subsidence	
	Epoch 3			Mila Fm.	Acritarch Ass. Zone I-II		
		Epoch 2					
	Terreneuvian			Lalun Fm.			
				Zaigun Fm.			
			Barut Fm.				
	541 Ma		Soltaniaeh Fm.		Massive post rift - Continental sediments		
					Hormuz salt		
						INTRA-CRATONIC	

**Fig. II.3:** Biozonation and tectonic events in Palaeozoic succession in the Zagros area. Showing summarized the known stratigraphic range of acritarch assemblages and species from Cambrian up to Permian deposits and synthesis of the main proposed controlling factors at the origin of the sedimentation and unconformities for the Palaeozoic of Zagros area.

## II.2. Conceptual methods

### II.2.1. Facies interpretation

Detailed sedimentological analysis of the lithology (texture and composition), geometry, sedimentary structures, gamma-ray log interpretation, clay minerals with using of X-Ray diffraction, palaeocurrent pattern, stratal stacking relationship and major surfaces in the field, resulted in the identification of several facies. The major controls of sediment architecture are discussed on the basis of the lithofacies and petrofacies characteristics and the nature of sedimentary cycles (Miall, 1996) as well as some facies classification and coding system. Folk's (1974) classification is used for sandstones and Dunham (1962) classification for carbonate rocks.

Five facies tables for Palaeozoic Formations (Seyahou, Dargaz, Sarchahan, Zakeen and Faraghan) are defined based on the combination of field observations and laboratory studies. The facies are grouped to facies association considering being genetically or environmentally related (Reading, 1996). The depositional profiles for each Formation illustrate the idealized distribution of the facies.

### II.2.2. Sequence stratigraphy

Sequence stratigraphy is a main and widely used method of stratigraphic analysis that can be applied to build frameworks of sequences, systems tracts and bounding surfaces at different scales of observation, depending on the purpose of the study and on the data available (Catuneanu et al., 2013).

Although in the model of Catuneanu et al. (2002), five systems tract are defined by the relative sea level changes, two are adapted to the depositional system of the study areas. The transgressive systems tract (TST) is bounded by the maximum regressive surface and sequence boundary at the base, and by the maximum flooding surface at the top. This systems tract forms when base level rise, and the rates of rise is more from the sedimentation rates. The highstand systems tract (HST) is bounded by the maximum flooding surface at the base, and by a composite surface at the top that includes the subaerial unconformity, the regressive surface of marine erosion, and the basal surface of forced regression. It corresponds to the late stage of base level rise during which the rates of rise drop below the sedimentation rates, generating a normal regression of the shoreline.

The maximum flooding surface (MFS) separates retrograding strata below from prograding strata above. The change from retrogradational to overlying progradational stacking patterns takes place during continued base level rise at the shoreline, when the sedimentation rates start to outpace the rates of base level rise (Catuneanu et al., 2006). Development of bioturbation, deep marine deposits and high gamma ray peak are indicators used for determination of transgressive surface and maximum flooding surface.

Based on depositional environments, stratigraphic position and results from previous palynological study, the Palaeozoic successions are described in depositional sequences.

In addition to the sedimentological characteristics of the facies, distinct erosional surface and gamma ray peaks used to determination of main sequence boundaries (SB).

Gamma-ray (GR), Uranium (U), Potassium (K) and Thorium (T) logs were used to trace sequence boundaries and maximum flooding surfaces for the surface sections. The most common petrophysical log types that are routinely used in this study for wells are gamma ray, sonic and neutron logs. Gamma ray logs are much more utilized in this study than the others, thus characterizing the lithology mostly within siliciclastic domains. The Gamma ray curve reflects the degree of radioactivity in response to the shaliness of the rocks or their organic content (Reader, 1993).

In comparison between my work and result with the chart proposed by Sharland et al., (2001), the sequence stratigraphic and chronostratigraphic interpretation is supported by a tectonostratigraphic review of the Arabian plate, and the identification, dating and correlation of Maximum Flooding Surfaces (MFS) (Fig II.4). However, the small difference between Zagros and Arabian Plate will be discussed in chapter 5. In the Zagros area, as a part of the Arabian Plate, sedimentary record developed through a series of major tectonic phases. The sedimentary cover was deposited during a late Precambrian to mid-Permian intra-cratonic phase, its tectonostratigraphic megasequences (TMS) and Maximum Flooding Surfaces (MFS) show in Fig II.4 (Sharland et al., 2001).

ERA	PERIOD	EPOCH	STAGE	Maximum flooding surfaces-AP Boundary				
				Preservation				
(Gradestein et al., 2012)				3	2	1		
PALEOZOIC	252.2 Ma <b>Permian</b>	Late	Changhsingian			AP6		
			Wuchiapingian					
		Middle	Capitanian					
			Wordian					
			Roadian					
			Kungurian					
	Early	Artinskian	P10	AP5				
		Sakmarian						
	298.9 Ma <b>Carboniferous</b>	Pennsylvanian	Asselian			AP4		
			Gzhelian					
			Kasimovian					
			Moscovian					
			Bashkirian					
		Mississippian	Serpukhovian					
			Visean				C10	
		358.9 Ma	Turnaisian					D30
		419.2 Ma <b>Devonian</b>	Late				Famennian	
	Frasnian							
	Middle		Givetian					
			Eifelian	D20				
	Early		Emsian	D10				
			Pragian					
Lochkovian	S20							
443.8 Ma <b>Silurian</b>	Pridolian			S10				
	Ludlowian							
	Wenlockian							
	Liandoverian							
485.4 Ma <b>Ordovician</b>	Late	Hirnantian			AP2			
		Katian						
	Sandbian	O40						
	Middle	Darriwillian				O30		
		Dapingian						
Early	Floian	O20						
Tremadocian	O10							
541 Ma <b>Cambrian</b>	Furongian		Cm30					
			Cm20					
	Epoch 3							
	Epoch 2							
Terreneuvian		AP1						

**AP**= Arabian Plate megasequence

— Arabian Plate tectonostratigraphic megasequences boundary

— Maximum flooding surface

Preservation= Estimated current preservation of MFS within area of present day sedimentary record

1= Plate-wide preservation, >75% coverage

2= Sub-regional preservation, 25%-75% coverage

3= Local preservation, <25% coverage

**Fig. II.4:** Chrono-sequence stratigraphy of the Palaeozoic succession of the Arabian Plate (Sharland et al., 2001). In Zagros, the sequence stratigraphic and chronostratigraphic interpretation is supported by a tectonostratigraphic review of the Arabian plate, and the identification, dating and correlation of Maximum Flooding Surfaces (MFS).